J Geophys (1984) 55:203-213

Journal of Geophysics

Bimodal induction in non-uniform thin sheets: do the present algorithms work for regional studies?

Marianne Mareschal and Guy Vasseur

Centre Géologique et Géophysique, Université des Sciences et Techniques du Languedoc, 34060 Montpellier Cedex, France

Abstract. Two algorithms presently exist which describe bimodal induction in non-uniform thin sheets on regional scales. One is due to Vasseur and Weidelt (1977), the other to Dawson and Weaver (1979). Their respective theoretical and numerical bases are examined and their performances critically tested on a variety of synthetic and regional models. We conclude that even though the algorithm proposed by Vasseur and Weidelt is much simpler than that of Dawson and Weaver, there is very little qualitative difference between the results which the corresponding programs produce. Occasional quantitative differences are observed which reflect the differences in numerical procedures.

Key words. Bimodal induction – Non-uniform thin sheets – Three-dimensional modelling – Current deviation

Introduction

The problem of what we will loosely call "current channelling" has given rise to considerable controversies and confusion in the recent past (e.g. Vasseur and Weidelt, 1977; Dawson and Weaver, 1979; Summers, 1981, 1982; Dupis and Thera, 1982; Le Mouël and Menvielle, 1982; Hebert, 1983; Wolf, 1983; Fischer, 1984; McKirdy and Weaver, 1984).

Jones (1984), in an excellent review of the topic, states that "in the real earth there are no such entities as 2D anomalies, all anomalies are 3D. Accordingly, the re-arrangement of lines of current density to the new 'equilibrium' is taking place in all anomalies, and, as such, must be given due consideration in any and every interpretation." This statement reflects exactly our own opinion on the matter.

Clearly, before trying to arbitrate whether the currents flowing through a region are more "locally induced" or more "forced through" by specific lateral conductivity contrasts, one should make certain that both effects can be modelled accurately, i.e. that proper tools exist which allow the modelling of disturbed skin effects as well as induction in three-dimensional bodies.

When the conductivity anomalies are confined to a superficial layer whose thickness is much smaller than the depth of penetration of the source field, the theoretical treatment of a three-dimensional problem can be greatly simplified by modelling the non-uniform layer as a thin sheet of variable conductance (Price, 1949). Charges accumulated at conductivity discontinuities definitely affect the local electric field (Price, 1973). For global problems, such as induction in the oceans, the deviated currents may be constrained to flow within horizontal loops only (e.g. Hobbs, 1971; Hobbs and Brignall, 1976) even though truly realistic models consider electrical contact between the earth and the oceans (Hewson-Browne and Kendall, 1981). In regional studies, particularly those involving the vicinity of islands, coastlines and channels, the current flowing in and out of the thin sheet can never be neglected (e.g. Ranganayaki and Madden, 1980), that is to say, both poloidal and toroidal current modes must be considered.

Two algorithms presently exist which take advantage of the thin sheet approximation and satisfy these conditions for the regional case: the method first introduced by Vasseur and Weidelt (1977), based on Weidelt's (1975) theory of induction in three-dimensional structures, and the method of Dawson and Weaver (1979), based on a generalization of the two-dimensional theory of Green and Weaver (1978). Both algorithms have been applied to a variety of real and synthetic models (Vasseur and Weidelt, 1977; Weidelt, 1977; Mareschal and Vasseur, 1983; Jones and Weaver, 1981; Weaver, 1982; McKirdy and Weaver, 1984), while the former has also been used to "remove" the effect of superficial current concentration in order to expose the deeper anomalies of a region (e.g. Menvielle and Rossignol, 1982; Menvielle et al., 1982; Tarits and Menvielle, 1983; Menvielle and Tarits, 1984).

These two algorithms, which differ in a variety of theoretical and numerical details, being based, nevertheless, on the same fundamental idea (the thin sheet approximation), can be cross-checked for consistency. Obviously, a necessary condition for their "automatic" usage when 1-D or 2-D models fail to satisfy field observations is that either they give similar answers to similar 3-D problems or if they do not, the conditions under which they differ are clear to the user's mind. A systematic comparison of the performances, advantages and disadvantages of the two methods is therefore given in the following sections.

Offprint requests to: M. Mareschal

We start by examining in detail the theoretical and numerical bases of the two formulations. We then apply the algorithm of Vasseur and Weidelt to a synthetic model similar to the model presented by Dawson and Weaver (1979) for long periods and to Weaver's (1982) model of Scotland for short periods. We conclude by considering a variety of channel models, using constraints that could be applied to the controversial Rhinegraben, and compare the results to those of McKirdy and Weaver (1984).

The integral equation

The cornerstone of the theoretical works considered here is the resolution of an integral equation for the surface electric field ($\mathbf{E}_s$) over the thin sheet. Once $\mathbf{E}_s$ is determined, a straightforward calculation gives the other components of the surface electromagnetic field. Both pairs of authors obtain their integral equation via Maxwell's equations, supplemented by boundary conditions across the thin sheet (continuity of the horizontal electric and vertical magnetic fields, discontinuity of the horizontal magnetic field), and solve the combined set by the method of Green's functions.

Vasseur and Weidelt define their Green's function in terms of the poloidal and toroidal vector fields that a horizontal electric dipole placed in a uniform sheet creates in its neighborhood, i.e.

$$\mathbf{G}_k = \mathrm{curl}^2(\hat{z} P_k) + \mathrm{curl}(\hat{z} T_k), \qquad (k = x, y, z)$$

and satisfies

$$\mathrm{curl}^2 \mathbf{G}_k(\mathbf{r}|\mathbf{r}_0) + \theta_n^2(\mathbf{r}_0)\, \mathbf{G}_k(\mathbf{r}|\mathbf{r}_0) = \hat{i}_k\, \delta(\mathbf{r}_0 - \mathbf{r}),$$
$$(\theta_n^2(\mathbf{r}) = i\omega\mu_0\sigma_n(\mathbf{r}))$$

outside the thin sheet. [The equivalent expression within the thin sheet is given by their Eq. (2.11).]

Since the poloidal mode eventually leads to the anomalous electric field driving vertical currents (the toroidal mode drives the horizontal currents), the coupling between the non-uniform sheet and any conductor underlying it is assured. In practice, $\mathbf{G}_k(\mathbf{r}|\mathbf{r}_0)$ is uniquely defined by the fact that the scalars P and T both satisfy a differential equation of the type $(\nabla^2 - \alpha^2) F = 0$ within uniform layers plus disjoint boundary conditions at the interfaces. The second rank tensor $\mathfrak{G}(\mathbf{r}|\mathbf{r}_0)$ appearing in their integral equation is then simply defined by:

$$\mathfrak{G}(\mathbf{r}|\mathbf{r}_0) = \sum_{i=1}^{3} \hat{x}_i\, \mathbf{G}_i(\mathbf{r}|\mathbf{r}_0)$$

Dawson and Weaver start by separating the electromagnetic field into its 6 scalar components, each one of which satisfies a differential equation of the type: $(\nabla^2 - \alpha^2)\, F = 0$. They then define their Green's function as the scalar satisfying

$$(\nabla^2 - \alpha^2)\, G_j(\mathbf{r}|\mathbf{r}_0) = \delta(\mathbf{r} - \mathbf{r}_0)$$

subject to

$$j G_j(x, y, \pm 0 | x_0, y_0, z_0) + (j-1)\, \frac{\partial G_j}{\partial z}(x, y, \pm 0 | x_0, y_0, z_0) = 0$$

where $j=0$ and $j=1$ correspond respectively to the Green's function obeying homogeneous Neumann or Dirichlet boundary conditions above ($z = -0$) or below ($z = +0$) the thin sheet. The solutions are matched across the thin sheet using the conditions of field (dis)continuity at the interface and are easily expressed in terms of algebraic expressions with exponential damping factors. The explicit use of individual Maxwell equations to define the horizontal magnetic field just above and under the thin sheet allows them to define the second rank tensor $\mathbf{K}(\mathbf{r}_0|\mathbf{r})$ appearing in their integral equation in terms of various components of their Green's function $\mathbf{G}_k(\mathbf{r}_0|\mathbf{r})$. It is the fact that they explicitly use $\mathrm{div}\, \mathbf{E} = 0$, i.e.

$$\frac{\partial E_z}{\partial z} = -\frac{\partial}{\partial \mathbf{r}} \cdot \mathbf{E}_s,$$

in their derivation of $\mathbf{K}$ that compels the coupling of the thin sheet to the underlying medium and thus allows vertical current flow.

It is clear that Vasseur and Weidelt have selected an approach which stresses the physics of the problem more than that of Dawson and Weaver. However, the major difference between the two theoretical methods resides in the basic setting of the problem.

Vasseur and Weidelt choose to separate the field into normal and anomalous contributions, the anomalous region of conductance $\tau_n + \tau_a$ (i.e. that part of the thin sheet giving rise to the anomalous field) being entirely surrounded by a region of normal conductance. Therefore, $\tau_a = 0$ everywhere outside the anomalous domain. The advantage of such a formulation appears as soon as one considers their integral equation in $\mathbf{E}_s$:

$$\mathbf{E}_s(\mathbf{r}_0) = \mathbf{E}_{ns}(\mathbf{r}_0) - i\omega\mu_0 \int \tau_a(\mathbf{r})\, \mathbf{E}_s(\mathbf{r})\, \mathfrak{G}(\mathbf{r}|\mathbf{r}_0)\, dS,$$

where it is clear that the integration has to be performed over the anomalous domain alone. Everywhere else $\tau_a = 0$.

Dawson and Weaver solve a more general problem for which the only constraint on the configuration of the anomalous domain is that:

$$\partial\tau/\partial x \to 0 \quad \text{as } |x| \to \infty$$

and

$$\partial\tau/\partial y \to 0 \quad \text{as } |y| \to \infty.$$

They choose to study the total field rather than its individual normal and anomalous parts and their integral equation (here taking the inducing field in the y-direction):

$$\{1 - i + 2\tau(\mathbf{r})\}\, \mathbf{E}_s(\mathbf{r}) = \hat{x} - \frac{i}{2\pi} \int_{-\infty}^{+\infty} \{\mathbf{K}(\mathbf{r}_0|\mathbf{r})\} \cdot \{\mathbf{E}_s(\mathbf{r}_0) - \mathbf{E}_s(\mathbf{r})\}\, dS$$

requires a surface integration over the whole thin sheet.

Note that both methods, since they are based on the thin sheet approximation, are only valid if the thickness of the surface layer is small when compared to the skin-depth of the underlying medium (to the first order) as well as in comparison to the skin-depth of the

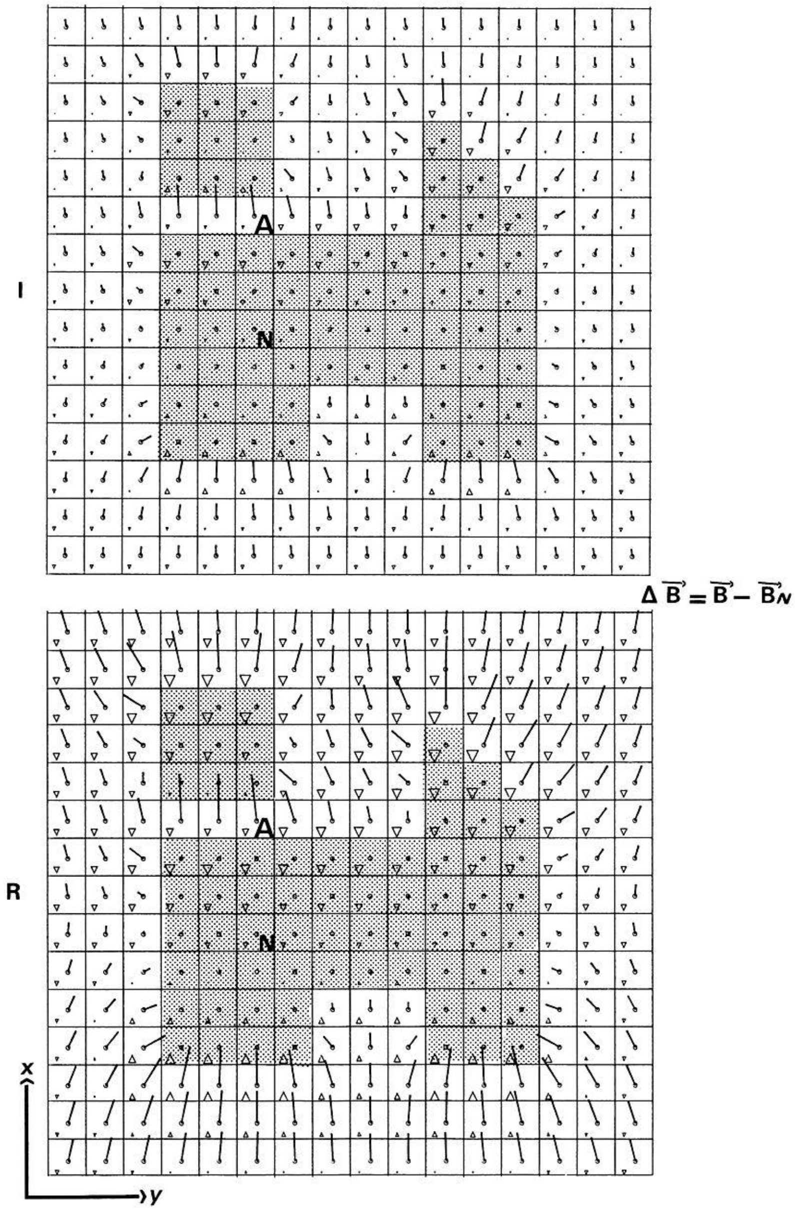

Fig. 1. Plots of the real and imaginary anomalous B-field for a unit normal field. In each cell, the horizontal component of $\Delta\mathbf{B}$ is proportional to the length of the line. The vertical component is given by a triangle pointing up or down and whose area is proportional to ΔB_z. The *shaded area* corresponds to the land. $T = 2$ h

material of the surface layer itself (to the second order), (e.g. Schmucker, 1970; Weaver, 1973). It is only in this case that the electric field is approximately constant across the thin sheet. These conditions are verified by the models that we present in later sections.

Numerical considerations on the resolution of the integral equation

It must be evident, from the theoretical development outlined above, that the policy followed by Vasseur and Weidelt is one of maximum simplicity, even at the price of introducing potentially unrealistic constraints (i.e. the anomalous domain must be entirely surrounded by a region of normal conductivity) whilst Dawson and Weaver's is one of greater generality, leading eventually to large consumption of computer time.

The same trends are observed in the numerical setting of the problem. Vasseur and Weidelt decompose their anomalous domain (comprised within a square or a rectangle) into a set of N squares within which $\mathbf{E}_s$ and τ_a are assumed to be constant. Therefore, the integration is performed on the tensor kernels alone and is independent of the superficial conductivity distribution. The system is solved iteratively by means of the Gauss-Seidel method which, at long periods (when the poloidal mode dominates over the toroidal), requires only a few iterations (usually less than 10).

Dawson and Weaver also use a grid (which in this case must be square) but provide the conductances at each node of the mesh rather than within the various cells. Again, the conductivity does not appear directly inside the integral and thus the numerical integration of the Green's kernels can be performed once per grid, regardless of the superficial conductivity subsequently selected (assuming, of course, that the underlying medium remains the same). Here, $\mathbf{E}_s$ is assumed to vary linearly in the x- and y-directions from node to node. The iterative method selected to solve the integral equation is that of Jacobi, supplemented by the spec-

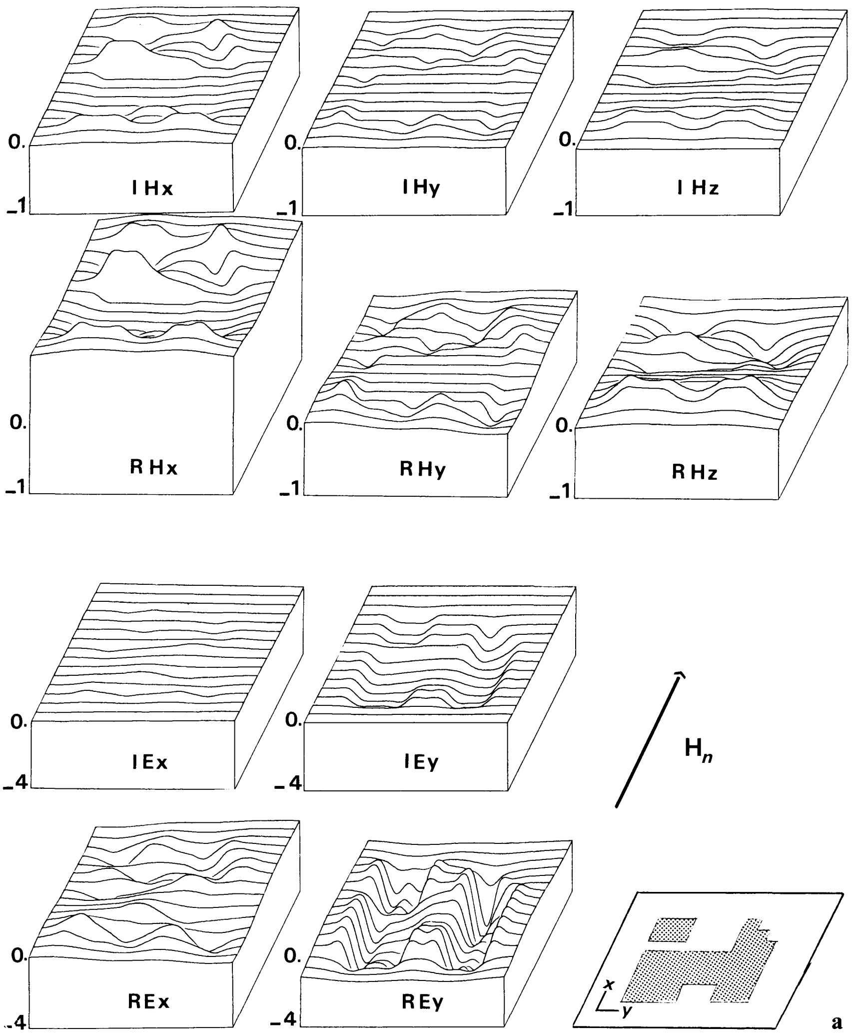

Fig. 2a and b. Block diagrams showing the traverse plots of 5 electromagnetic components of the total field generated by **a** a unit normal field along Ox and **b** a unit normal field along Oy. $T = 2$ h

trum displacement technique introduced by Hutson et al. (1972), thus allowing the introduction of an arbitrary parameter which insures convergence at certain conductance values. The method of shifting the spectrum extends the range of convergence to high frequency and/or high conductivity contrasts. However, the Jacobi iteration scheme in itself has much slower rates of convergence than the Gauss-Seidel method. It is for that reason that Weaver (1982) rewrote the iterative scheme in Gauss-Seidel form for his model of Scotland.

The major difficulty encountered by both procedures is the handling of the singular cell or node, i.e. of that point where $\mathbf{r} = \mathbf{r}_0$ in the Green's dyad. There, the Green's function must be extrapolated from its value at neighbouring points. This task is easily achieved in the Vasseur-Weidelt formalism due to their simplifying assumption of constant $\mathbf{E}_s$ within each individual cell (and also because they replace the square cell by a circular disk of equal area in order to evaluate the integral). It is more difficult for Dawson and Weaver, especially when the singular nodes lie on the boundary of the grid. In such cases, they have to assume that the conditions at infinity are already applicable, i.e. that the normal conductance gradient is nil. Furthermore, since Dawson and Weaver work in terms of total fields, their integration has to be performed on an infinitely large sheet, i.e. over the external domain as well as the purely anomalous region.

However, once again, Vasseur and Weidelt must pay a price for their computational simplification. The fact that their $\mathbf{E}_s$ remains constant within an individual cell prevents them from modelling small-scale anomalies with a reasonable grid size (remember that their anomalous domain must always be surrounded by a "normal" region), as they already noted in their model of the Pyrenees (Vasseur and Weidelt, 1977). But it should be noted that the linear variation that Dawson and Weaver select for $\mathbf{E}_s$ does not allow them much more flexibility in the modelling of small-scale anomalies. Their singular mode calculations on the boundaries, coupled to the fact that their grid must remain square and thus rapidly increases in size if conductivity discontinuities have to be contained well within the edges of the anomalous domain, can also lead to relatively severe constraints (e.g. McKirdy and Weaver, 1984).

A synthetic model

The model considered in this section is shown as part of Fig. 1. It consists of a pseudo-island and continent ($\tau = 500$ S). It includes a channel, a bay and a peninsula

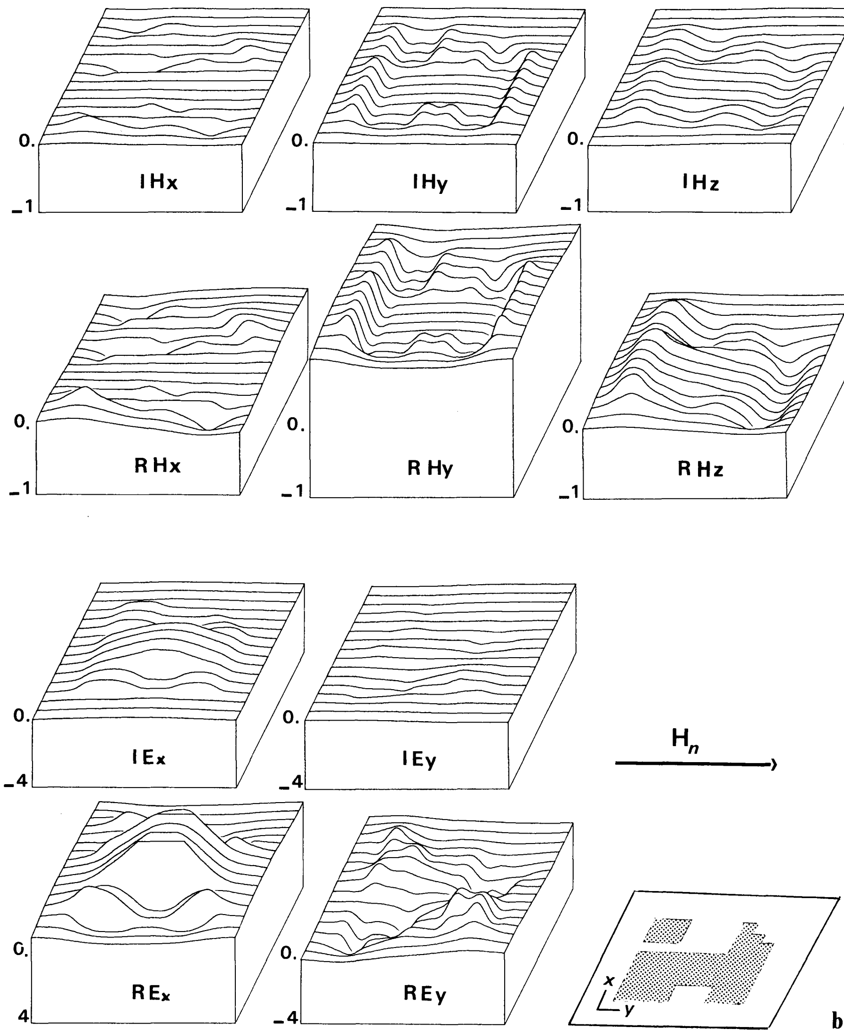

($\tau = 8{,}000$ S) and is similar in principle to the synthetic model presented by Dawson and Weaver (1979). The source period is 2 h and the anomalous domain is entirely contained within a 10×10 grid (elementary cell $= 50 \times 50\ \mathrm{km}^2$).

Since several members of the induction community are of the opinion that current deviation is best evidenced by the differential sounding method introduced by Babour and Mosnier (1977), our first figure is chosen to represent the difference field $\Delta\mathbf{B} = \mathbf{B} - \mathbf{B}_N$, where $\mathbf{B}_N$ stands for the field at a reference ("normal") station (not to be confused with what is called, in our formalism, a cell of normal conductivity, i.e., in this case, a water cell!). For this figure, the magnetic source field is in the x-direction and thus induces current through the channel, as is clearly indicated by the large ΔB_x component and the reversal in ΔB_z (best seen in the imaginary component). Note how current deviations around the various other land features also affect the direction of horizontal $\Delta\mathbf{B}$ and cause changes in the sign of ΔB_z.

When the source field is in the y-direction (figure not shown here), all current flowing through the channel must be due to deviation. This amount of current is not negligible, as can be seen, for instance, by comparing the B_x field generated in cell A by a unit normal field at N parallel to Ox, i.e. $B_x(A) = 0.40\,\mathrm{e}^{i\,30^\circ}$ (instead of $B_x(A) = 0$ as would be expected in the absence of deviation), to the same component in the same cell generated by a unit normal field at N parallel to Oy, i.e. $B_x(A) = 1.92\,\mathrm{e}^{i\,0^\circ}$.

Figures 2a and b give the traverse plots of the three components of the total magnetic field as well as of the two horizontal components of the total electric field for the inducing magnetic field polarized either in the x (Fig. 2a) or y (Fig. 2b) direction. As already pointed out by Dawson and Weaver, the main current flow being in a direction perpendicular to that of the inducing magnetic field, the large changes in magnitude of the horizontal electric field, at boundaries perpendicular to that flow, are due to the build-up of charges on the sea-land boundary. These serve to deflect the current around the obstacle and thus generate electric fields parallel to the magnetic field of the source. This pattern is noticeable in the H field plots, too, where large variations are observed in the horizontal component of H perpendicular to all boundaries parallel to the main current flow. At those boundaries, horizontal magnetic components in the direction of the main current flow, as well as reversals in the vertical component, can be recognized.

Dawson and Weaver (1979) did not consider the magnetic response of their model but did calculate E_z just below the thin sheet (that E_z correlates directly

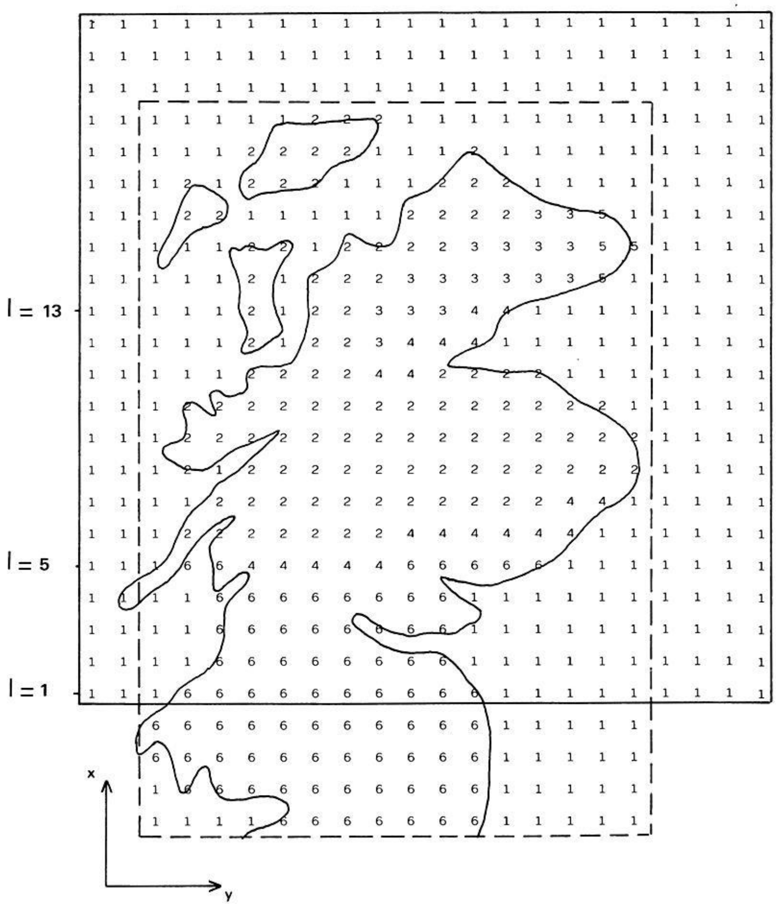

Fig. 3. The conductance model of Scotland: (1) 720.0 S (shallow sea-water), (2) 1.6 S (Lewisian foreland), (3) 5.6 S (Northern Scotland), (4) 80.0 S (Great Glen and Highland Boundary faults), (5) 56.0 S (sedimentary cover), (6) 8.0 S (Borders). The *square* corresponds to Weaver's grid, the *rectangle* to ours (M − V). Profiles number 1, 5 and 13, used in Figs. 4 and 5, are defined

with the vertical deviations of current at sea-land boundaries), which clearly indicates the presence of vertical currents at boundaries perpendicular to the main current flow. Vasseur and Weidelt do not calculate that component (although it could be easily added to their algorithm) but simple inspection of their Figs. 2(a, b) readily gives a qualitative corroboration of Dawson and Weaver's results. Indeed, these figures show that at the crucial boundaries, $\partial E_y/\partial y$ does not always compensate $\partial E_x/\partial x$ and thus a $\partial E_z/\partial z$ must exist (which is not entirely due to the effect of surface charges) to satisfy $\nabla \mathbf{E} = 0$.

Even though Dawson and Weaver's synthetic model was only introduced as an aside to the theory and therefore was not thoroughly discussed (only one source polarization was considered, and no mention was made of the magnetic field), its response seems to be extremely consistent with the response of our model. At this scale, the fact that Vasseur and Weidelt keep $\mathbf{E}_s$ constant within each individual cell does not seem to affect the results. Of course, in this specific example, the fact that they have to surround their anomalous domain by normal features is an advantage, since it gives us more boundaries to analyse! Its effect on a more realistic model, i.e. the model of Scotland, is examined in the next section.

A model of Scotland

Hutton et al. (1981) recently summarized the results of induction studies in Scotland and presented a two-dimensional geoelectric model which best satisfies the observations. The complexity of their model soon led Weaver (1982) to attempt some three-dimensional modelling of the region with the thin sheet approximation. He devised a conductance model which, he felt, would best represent the lateral variations of the integrated conductivities suggested by Hutton and coworkers. This is the model of Scotland considered here to test the performances of the algorithm defined by Vasseur and Weidelt. However, before proceeding to any comparison, it is important to keep in mind that the conductance models used by the two different algorithms are identical only in appearance: indeed, since the same values of conductance are given in Dawson and Weaver's algorithm at *point* nodes of the mesh while in the Vasseur and Weidelt's algorithm, they are given at the centre of *square* uniform cells, the conductance contours are not superposable.

To satisfy the thin sheet conditions with the conductances selected and the grid chosen (22×22 cells, each representing $20 \times 20\ \mathrm{km}^2$), Weaver had to limit the source period to 25 s. Because of the algorithm he uses, he also had to define his "anomalous" square as being large enough to cover the whole of Scotland plus a sufficient area of surrounding seas in order to keep sharp variations in conductance perpendicular to a boundary well away from the edges of the grid. That problem does not exist in the Vasseur-Weidelt algorithm for which the grid may be the smallest rectangle overlapping the purely anomalous domain. However, since the algorithm assumes the anomalous region to

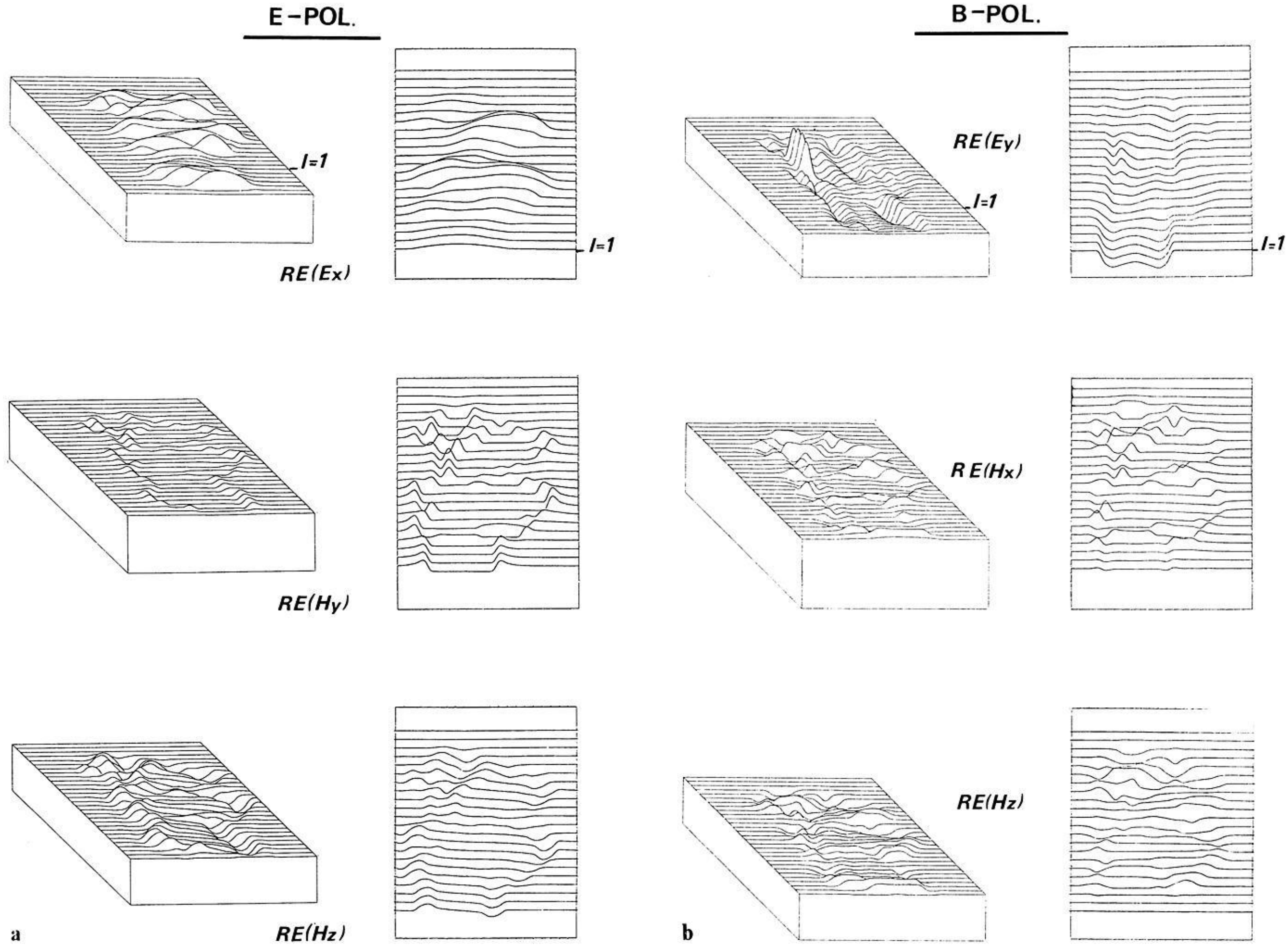

Fig. 4a and b. Traverse plots comparing the qualitative behaviour of Weaver's (*right*, $T=25$ s) and our results (M−V, *left*, $T=30$ s). Individual scales vary from one component to another. **a** (*E*-pol.) unit normal field along Oy, **b** (*B*-pol.) unit normal field along Ox

be entirely surrounded by normal structure (here, the seas), we had to lower the southern border of Weaver's grid to northern England where the presence of a ficticious sea would not affect the Scottish results. Our model is thus made of 23×16 elementary square cells, still slightly smaller than Weaver's original, as clearly appears in Fig. 3 where the details of the selected structure are defined. Note, however, that for the conductances and convergence criterion selected in the Gauss-Seidel iterative scheme, a period of 25 s is below the threshold that our algorithm can handle without diverging. We have thus run our model at 30 s.

Figure 4a presents traverse plots produced by our model (*left*), as well as the equivalent profiles generated by the algorithm of Dawson and Weaver (*right*). Since this figure corresponds to an *E*-polarization regional field (i.e. its source is along Oy), we have chosen to depict Real(E_x) and Real(H_y) which are the dominant components of the electromagnetic field. We include the variations of the vertical magnetic component (real part) since it is indicative of the coast effect and actually reproduces almost exactly the shape of the coast line. Note that in this figure, Weaver's profiles represent variations of the field component while our block diagrams are representative of total components. The same is true for Fig. 4b which gives the corresponding curves for a *B*-polarization. In this case, we represent Real(E_y) and Real(H_x). The in-phase component of the vertical magnetic field is still presented even though it is less representative of the coast effect than in the *E*-polarization, the main flow of current being more perpendicular than parallel to most of the coastlines. We did not deem it necessary to present the whole set of profiles for each component since there is virtually no qualitative difference between our results and Weaver's. Neither is the detailed signature of current deviation analysed here since it is thoroughly described by Weaver (1982).

Quantitative differences in the results are mostly due to the fact that our model is made of patches of constant conductance (and $\mathbf{E}_s$) while Weaver's allows for a linear variation between the grid nodes, smoothing out the response of the electromagnetic field. This is quite apparent in Fig. 5 where we consider two E_x profiles normalized to the same regional field (*E*-polarization) and compare Weaver's response to ours. The two profiles 13, which are taken along a band of conductance roughly reproduced in the coded profiles below the curves, are quite similar whilst the two profiles 5, taken along a sharp N−S conductance boundary, are quite different. Weaver's field is much more affected by the smoothing presence of the neighbouring cells

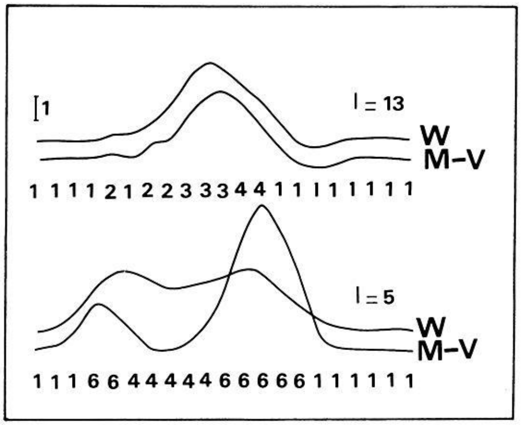

Fig. 5. E_x profiles (normalized to E_x (1, 1)) given by Weaver's (W, $T=25$ s) or our model (M – V, $T=30$ s). The conductance values are coded below the curves and have been defined in Fig. 3. The vertical scale is given by a unit displacement

than ours which follows almost exactly the underlying conductance structure, a possibly more realistic behaviour at the short periods considered here (for which even the resistive substratum – $\rho=1{,}000\,\Omega$m – has a skin depth of the order of only four cell widths).

Note also that our algorithm seems to generate larger quadrature magnetic components than Weaver's. In particular, we produce imaginary B_z components which can be larger than half the corresponding real components, a value never attained with Weaver's algorithm (see Fig. 6). If one of the effects of horizontal current deviation is to increase Imag(B_z) (e.g. Bailey and Edwards, 1976), then this observation might again simply be due to the fact that we do not smooth out the effects of any structure and thus eventually reinforce channelling.

Naturally, our larger quadrature B_z components also give us larger imaginary induction vectors than Weaver's (not shown here). Our real induction arrows, which include the effects of both E- and B-polarization, are compared in Fig. 7 to Weaver's and to the arrows calculated from field data at 23 s (Mbipom and Hutton, 1983). Even if our arrows can be said to differ very slightly from Weaver's, in that they tend to indicate high conductivity strips slightly better than his, the obvious message of Fig. 7 is that frequently neither his nor our vectors satisfy field observations outside the coastline stations. Our results are so similar to Weaver's that we will not discuss the implications of such a discrepancy, Weaver (1982) having presented a thorough discussion of the problem in his article. However, it seems to us that since the electrojet is known to return repeatedly to the same location (e.g. Mareschal, 1981), a recurrent source effect might be worth investigating at some inland stations.

Of channels and games

There is no doubt that the two algorithms considered in this article produce very similar results and that the pursuit of systematic comparisons on identical models will not throw much new light on the subject. We will simply conclude by presenting three synthetic models of "channels" which could satisfy the differential sounding observations along the Rhinegraben (summarized in Fig. 8a) and, at the same time, allow the study of interrupted, offset, or broken channels connecting two highly conducting regions (in this case, the German sedimentary basin to the north and the Mediterranean to the south?). The exercise is basically intended as a test on channel behaviour (and thus as a corroboration of McKirdy and Weaver's recent results) and does not pretend to arbitrate the long-lasting controversy excellently summarized by Jones (1984).

Since most arguments in favour of the three-dimensionality of an anomaly rely heavily on the results of differential sounding experiments (e.g. Babour and Mosnier, 1979), and since Menvielle and Tarits (1984) do not present any field difference maps in their recent re-examination of the Rhinegraben anomaly in terms of the thin sheet modelling, we present in Fig. 8 the difference fields $\Delta\mathbf{B}=\mathbf{B}-\mathbf{B}_N$ calculated at the centre of each cell ($100\times100\,\mathrm{km}^2$) of a 21×17 grid. Note that the data shown in Fig. 8a correspond to the small circled region only (Fig. 8b–d) and are thus too sparse to disprove any of the three models considered here.

In Fig. 8b, the channel is interrupted half-way be-

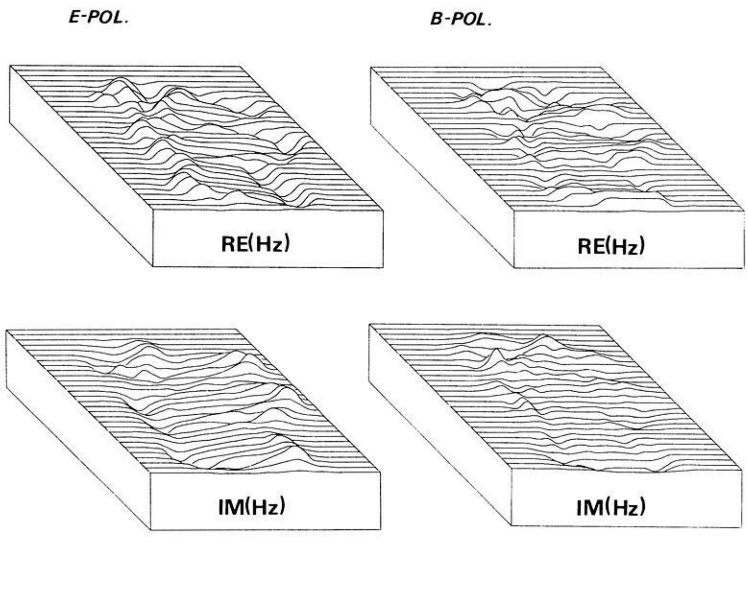

Fig. 6. The real and imaginary components of H_z total produced by a unit normal field either along Oy (E-pol.) or along Ox (B-pol.) with the algorithm of Vasseur and Weidelt. The four bloc diagrams are plotted on the same scale. $T=30$ s

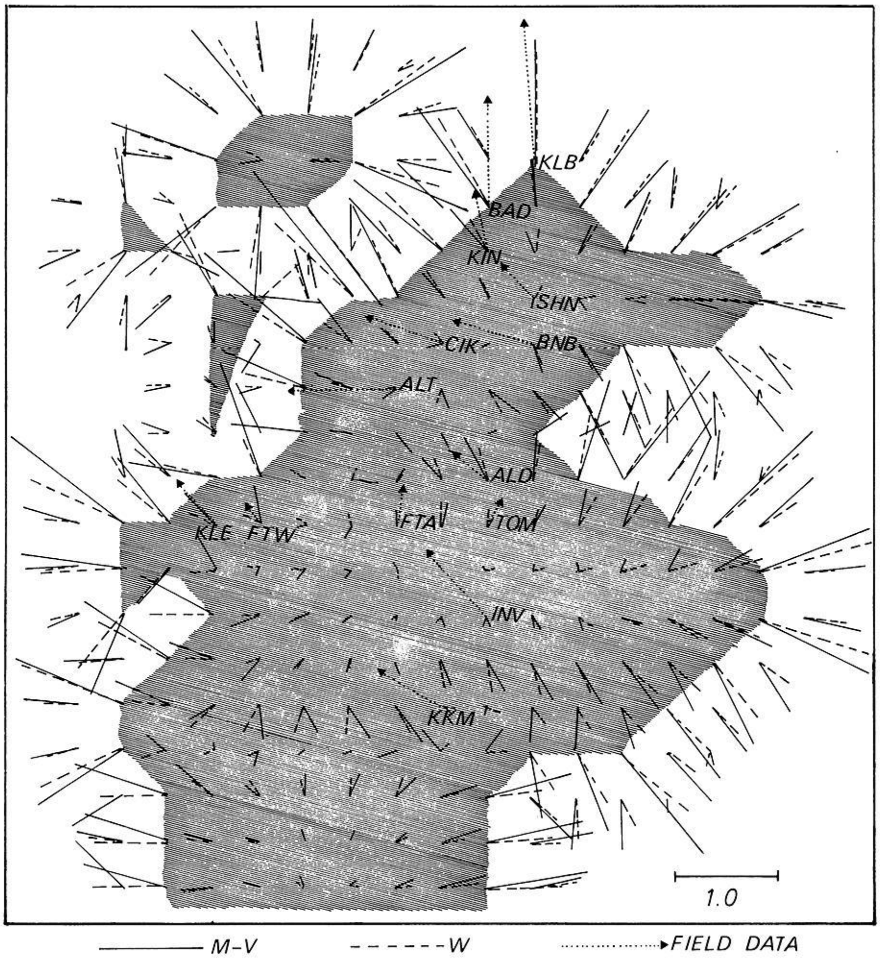

Fig. 7. Comparison of induction vectors given by Weaver's (W, $T=25$ s) and our model (M – V, $T=30$ s). We calculate the field at the centre of each cell, while Weaver calculates his at the nodes. His grid has thus been shifted to overlap ours, and the land contours given are Weaver's (*shaded area*). Field data (at 23 s) are also given at the grid point closest to their actual recording site

tween the two good conductors. The source polarization selected ($\mathbf{H}_N$ along Oy) naturally induces current through the channel, as indicated by the large difference fields and ΔB_z reversals between two adjacent cells. As expected with the algorithm of Vasseur and Weidelt, we only observe the effect of a channel interruption in the very last conductive cell, but nevertheless maintain a non-zero difference field in the four resistive cells connecting the channel to the Mediterranean Sea. In Fig. 8c, the channel is offset (by two cells only). It is for this model that the difference fields are largest. Note the deviation of current parallel to the magnetic source field along the path connecting the two half-channels. The signature of $\Delta\mathbf{B}$ in that region is identical to the signature presented by McKirdy and Weaver (their Fig. 6) who analysed a similar configuration at the short period of $T=10$ min. Finally, Fig. 8d shows that current is deviated in the direction of the magnetic source field even across a resistive cell connecting the two half-channels.

Again, our results are qualitatively very comparable to those presented by McKirdy and Weaver. Since their study was a thorough analysis of the channelling of induced currents between two oceans, we do not feel justified in reproducing their discussion. Simply note, however, how the behaviour of the difference field along the outline of the continents chosen in these three models is close to the behaviour noted in the section describing a synthetic model and clearly indicates deviation of current around land masses.

Conclusion

Do the algorithms work? Apparently, yes, and even give very similar answers to similar problems.

The most common argument against the algorithm of Vasseur and Weidelt is that it requires the anomalous domain to be entirely surrounded by a region of normal conductivity. We have shown, for the model of Scotland, that this was of very little consequence since (a) the anomalous domain could easily be extended in one direction without increasing the number of cells used by Dawson and Weaver (Vasseur and Weidelt can use a rectangular grid, Dawson and Weaver cannot), and (b) the effect of neighbouring cells is minimal in their algorithm.

Vasseur and Weidelt's program is definitely simpler and thus computationally faster than Dawson and Weaver's. However, since it does not integrate the effect of neighbouring cells in the calculation of $\mathbf{E}_s$, its response along a profile of variable conductance is not as smooth as Dawson and Weaver's (e.g. see Fig. 5). The algorithm has the further disadvantage, at present, of divergence for very short periods ($T \leqq 25$ s for conductances such as those used to model Scotland). On the other hand, Dawson and Weaver's algorithm is quite

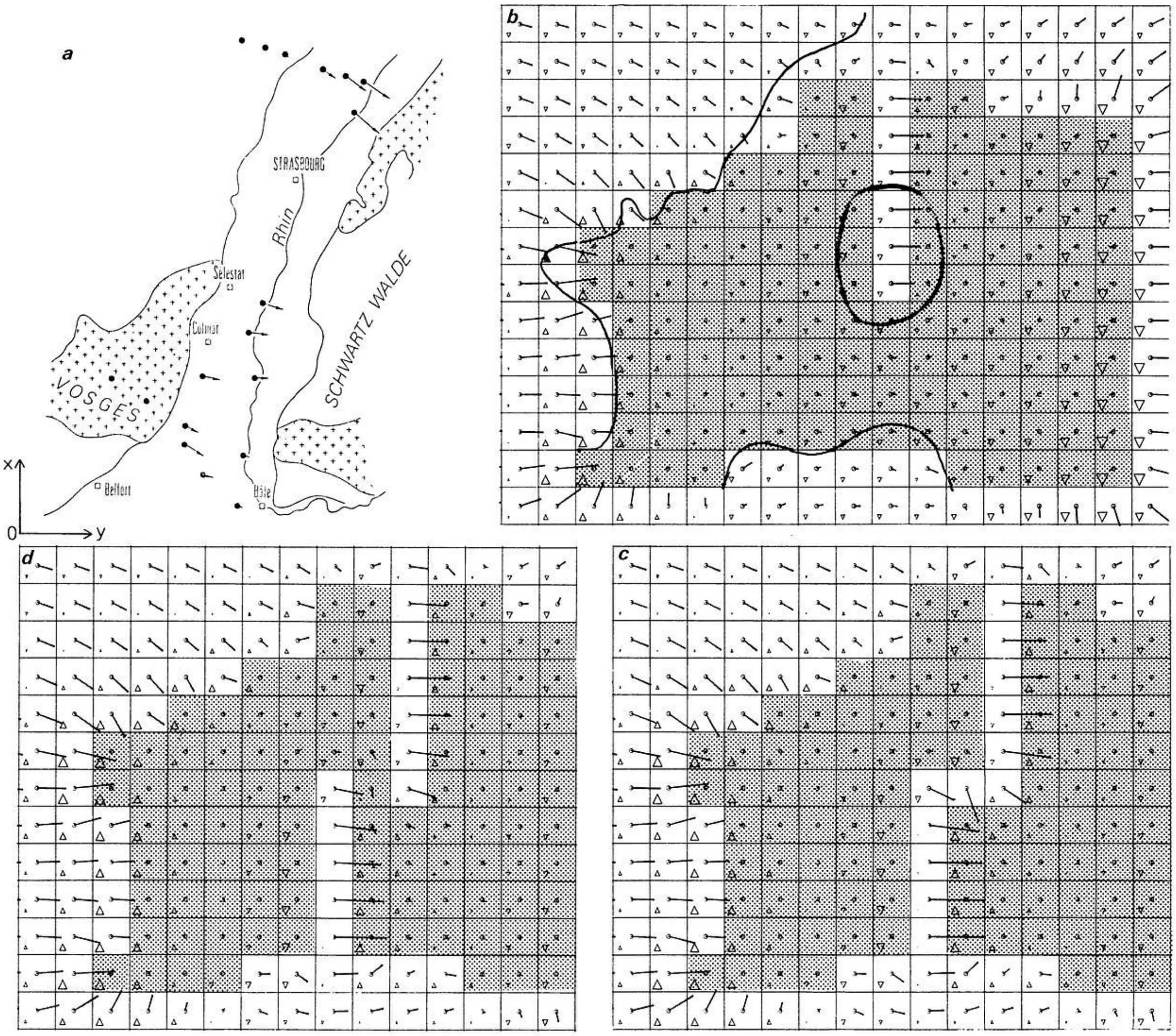

Fig. 8. Plots of the real anomalous $\Delta\mathbf{B}$-field over three possible models for the Rhinegraben. **a** the horizontal difference fields observed at substorm periods (after Babour and Mosnier, 1979; arbitrary units). **b, c** and **d** depict three different models for the conductivity structures. The region shown in **a** corresponds only to the circled region of **b**. The following parameters are chosen: $\tau_{\text{land}} = 500$ S, $\tau_{\text{conductor}} = 8{,}000$ S, $T = 2$ hours. No quantitative comparison is possible since the units used in **a** are not defined

elegant but cannot handle conductivity discontinuities (perpendicular to a boundary) close to the grid edges. Therefore, it usually requires the definition of a rather large anomalous domain. However, our comparison clearly shows that the points mentioned here introduce minor differences only between the performances of the two algorithms and thus do not warrant the preclusion of one approach against the other.

Acknowledgements. We thank John Weaver for providing us with his complete results concerning the model of Scotland. We are also grateful to Rosemary Hutton for sending us the detailed observations of the geoelectromagnetic measurements across Northern Scotland.

References

Babour, K., Mosnier, J.: Differential geomagnetic sounding. Geophysics **42**, 66–76, 1977

Babour, K., Mosnier, J.: Differential geomagnetic sounding in the Rhinegraben. Geophys. J.R. Astron. Soc. **58**, 135–144, 1979

Bailey, R.C., Edwards, R.N.: The effect of source field polarization on geomagnetic variation anomalies in the British Isles. Geophys. J.R. Astron. Soc. **45**, 97–104, 1976

Dawson, T.W., Weaver, J.T.: Three-dimensional induction in a non-uniform thin sheet at the surface of a uniformly conducting earth. Geophys. J.R. Astron. Soc. **59**, 445–462, 1979

Dupis, A., Thera, A.L.: Natural electromagnetism in the Rhinegraben. Geophys. J.R. Astron. Soc. **68**, 545–557, 1982

Fischer, G.: The north Pyrenean magnetic anomaly re-examined. Annales Geophysicae, in press 1984

Green, V.R., Weaver, J.T.: Two-dimensional induction in a thin sheet of variable integrated conductivity at the surface of a uniformly conducting earth. Geophys. J.R. Astron. Soc. **55**, 721–736, 1978

Hewson-Browne, R.C., Kendall, P.C.: Electromagnetic induction in the Earth in electrical contact with the oceans. Geophys. J.R. Astron. Soc. **66**, 333–349, 1981

Hebert, D.: The frequency response of the horizontal magnetic field for a conductive channel. Geophys. J.R. Astron. Soc. **73**, 577–580, 1983

Hobbs, B.A.: The calculation of geophysical induction effects

using surface integrals. Geophys. J.R. Astron. Soc. **25**, 481–509, 1971
Hobbs, B.A., Brignall, A.M.M.: A method for solving general problems of electromagnetic induction in the oceans. Geophys. J.R. Astron. Soc. **45**, 527–542, 1976
Huston, V.C.L., Kendall, P.C., Malin, S.R.C.: Computation of the solution of geomagnetic induction problems: a general method, with applications. Geophys. J.R. Astron. Soc. **28**, 489–498, 1972
Hutton, V.R.S., Dawes, G., Ingham, M., Kirkwood, S., Mbipom, E.W., Sik, J.: Recent studies of time variations of natural electromagnetic fields in Scotland. Phys. Earth. Planet. Inter. **24**, 66–87, 1981
Jones, A.G.: The problem of current channelling: A critical review. Geophys. Surveys, in press 1984
Jones, A.G., Weaver, J.T.: Induction by uniform and non-uniform fields over northern Scandinavia: Field data and numerical modelling. 4th IAGA assembly, Edinburgh, Scotland, 1981
Le Mouel, J.L., Menvielle, M.: Geomagnetic variation anomalies and deflection of telluric currents. Geophys. J.R. Astron. Soc. **68**, 575–587, 1982
Mareschal, M.: Source effects and the interpretation of geomagnetic sounding data at sub-auroral latitudes. Geophys. J.R. Astron. Soc. **67**, 125–136, 1981
Mareschal, M., Vasseur, G.: Bimodal electromagnetic induction in non-uniform thin sheets and application to Scotland. 18th IUGG General Assembly, Hamburg, Fed. Rep. Germany, 1983
Mbipom, E.W., Hutton, V.R.S.: Geoelectromagnetic measurements across the Moine Thrust and the Great Glen in northern Scotland. Geophys. J.R. Astron. Soc. **74**, 507–524, 1983
McKirdy, D., Weaver, J.T.: A numerical study of the channelling of induced currents between two oceans. J. Geomagn. Geoelectr., in press 1984
Menvielle, M., Rossignol, J.C.: Conséquences tectoniques de l'existence d'une anomalie de conductivité électrique au nord du Maroc. Can. J. Earth Sci. **19**, 1507–1517, 1982
Menvielle, M., Tarits, P.: 2-D or 3-D interpretation of conductivity anomalies: example of the Rhinegraben conductivity anomaly. Geophys. J.R. Astron. Soc., in press 1984
Menvielle, M., Rossignol, J.C., Tarits, P.: The coast effect in terms of deviated electric currents: a numerical study. Phys. Earth Planet. Inter. **28**, 118–128, 1982
Price, A.T.: The induction of electric currents in non-uniform thin sheets and shells. Quat. J. Mech. Applied Math. Vol. II, Pt. 3, 283–310, 1949
Price, A.T.: The theory of geomagnetic induction. Phys. Earth Planet. Inter. **7**, 227–233, 1973
Ranganayaki, R.P., Madden, T.R.: Generalized thin sheet analysis in magnetotellurics: an extension of Price's analysis. Geophys. J.R. Astron. Soc. **60**, 445–457, 1980
Schmucker, U.: Anomalies of geomagnetic variations in the Southwestern United States. Bull. Scripps. Inst. Ocean. **13**, 1–160, 1970
Summers, D.M.: Interpreting the magnctic fields associated with two-dimensional induction anomalies. Geophys. J.R. Astron. Soc. **65**, 535–552, 1981
Summers, D.M.: On the frequency response of induction anomalies. Geophys. J.R. Astron. Soc. **70**, 487–502, 1982
Tarits, P., Menvielle, M.: Etude du champ magnétique anormal d'origine intralithosphérique. Can. J. Earth. Sci. **20**, 537–547, 1983
Vasseur, G., Weidelt, P.: Bimodal electromagnetic induction in non-uniform thin sheets with an application to the northern Pyrenean induction anomaly. Geophys. J.R. Astron. Soc. **51**, 669–690, 1977
Weaver, J.T.: Induction in a layered plane-earth by uniform and non-uniform source fields. Phys. Earth Planet. Inter. **7**, 266–281, 1973
Weaver, J.T.: Regional induction in Scotland: an example of three-dimensional numerical modelling using the thin sheet approximation. Phys. Earth Planet. Inter. **28**, 161–180, 1982
Weidelt, P.: Electromagnetic induction in three-dimensional structures. J. Geophys. **41**, 85–109, 1975
Weidelt, P.: Numerical study of a conductive channelling effect. Acta Geodaet. Geophys. Montanist. Acad. Sci. Hung. tomus **12** (1–3), 195–205, 1977
Wolf, D.: Singular solutions to Maxwell's equations and their significance for geomagnetic induction. Geophys. J.R. Astron. Soc. **75**, 279–283, 1983

Received December 14, 1983; Revised version March 23, 1984
Accepted March 27, 1984